



Generalising Axion-like particle as the curvaton:

sourcing primordial density perturbation and non-Gaussianities

Anish Ghoshal ^{1,*} and Abhishek Naskar ^{2,†}

¹*Institute of Theoretical Physics, Faculty of Physics,
University of Warsaw, ul. Pasteura 5, 02-093 Warsaw, Poland*

²*Department of Physics, Indian Institute of Technology Bombay,
Mumbai 400076, India*

Abstract

We investigate the non-perturbatively generated axion-like particle (ALP) potential, involving fermions in the dark sector that couple to the ALP, in an early cosmological inflationary stage with the ALP being a spectator field. The potential here deviates from the standard cosine nature due to the presence of the two fermion masses m_u and m_d which couple to the ALP. The ALP is a spectator field during inflation but it starts to oscillate and dominates the energy density of the universe after inflation ends, thereby sourcing isocurvature perturbations, while standard curvature fluctuations from the inflaton are assumed to be sub-dominant. Subsequently the ALP decays converting the isocurvature perturbations to adiabatic perturbations thereby acting as the origin of the primordial density perturbations. We identify the parameter space involving the axion decay constant f_a , scale of confinement Λ , ALP mass m and the masses of the fermions, m_u and m_d where it can satisfactorily behave as the curvaton and source the observed primordial density perturbation. We also predict local non-Gaussianity signals for bi-spectrum and tri-spectrum f_{NL} and g_{NL} , as a function of the ratio m_u/m_d , which are within the allowed range in the latest Planck observations and are detectable with future observations. Particularly we observed that the value of f_{NL} and g_{NL} are dependent on the ratio of m_u and m_d : f_{NL} is more or less positive for all scenarios except $m_u = m_d$ and g_{NL} is always positive irrespective of the ratio between m_u and m_d . The results of our analysis in the limit $m_u = m_d$ resembles vanilla curvaton scenario while in the limit $m_u \gg m_d$ resembles pure axion cosine potential.

*Electronic address: anish.ghoshal@fuw.edu.pl

†Electronic address: abhiatrkm@gmail.com

I. INTRODUCTION

Even before the cosmological scales starts entering the Hubble horizon of the universe, the primordial curvature perturbation ζ is already present, at least few Hubble times before this. It must be during this era, and particularly on those scales, the Fourier components $\zeta(k)$ (k being momentum) are time-independent. They set the initial condition for the large-scale structure (LSS) formation in the Universe [1]. Therefore, $\zeta(k)$ is determined, leading to a direction of model-buildings in theoretical cosmology that lead to the origin of ζ .

Usually it is believed that the generation of $\zeta(k)$ presumably starts at the time of horizon exit during inflation (that is, when $k = aH \equiv \dot{a}$ where $a(t)$ is the FRW metric scale factor of the universe) when the vacuum fluctuation of one or more scalar (or vector [2]) fields takes the form of a classical perturbation. In a slow-roll inflationary model of early universe with a single-field ϕ_I , ζ is generated by the perturbation $\delta\phi_I$, which means that ζ is generated only at the time of horizon exit, and remains constant afterwards. On the other hand, another alternative and well-motivated scenario is the curvaton scenario [3], in which case ζ is now instead generated by the perturbation $\delta\sigma$ of a ‘curvaton’ field σ_c , that has practically no effect, or almost remains frozen during inflation. This means that σ_c generates ζ only and only when its energy density becomes significant, mostly when inflation has ended. One may also have mixed inflaton-curvaton scenario where both $\delta\phi_I$ and $\delta\sigma_c$ contributes significantly to ζ [4], ζ be generated during multi-field inflation, or via a ‘modulating’ field that induces an effective mass or coupling to be inhomogeneous [1].

In this paper, we will stick to purely the curvaton scenario however assuming single-field inflationary model to hold true. In our case we will look at make axion or axion-like particle as the curvaton. In context to the Standard Model (SM) of particle physics, something well-known as the The Strong CP problem is one of the unsolved problems; and it strongly recommends to go beyond the SM (BSM). The so-called Peccei-Quinn (PQ) mechanism [5, 6], with predictions of a light pseudo-Nambu-Goldstone boson (pNGB), famously called the QCD axion, dynamically addresses the strong CP phase $\bar{\theta}_{\text{QCD}}$ to be zero [7, 8]. Non-perturbative effects of QCD, under strong confining dynamics generates QCD axion mass which must be lighter than $\mathcal{O}(10)$ meV to satisfy the current astrophysical observational bounds [9–11]. (see Refs. [12–18] for reviews).

On the other hand, going beyond the standard QCD axion paradigm, we also envisage

several Axion-like particles (ALPs) that are also light gauge-singlet pseudoscalar bosons that couple weakly to the Standard Model (SM) and generically appear as the pseudo-Nambu-Goldstone boson (pNGB), particularly in theories with a spontaneously broken global $U(1)$ symmetry, and are motivated from various string theory constructions [19]. ALPs could solve some other open questions in the SM, such as the hierarchy problem of the Standard Model via the relaxion mechanism [20] responsible for inflationary cosmology [21–23], be non-thermal dark matter (DM) candidates [24–26], account for the dark energy in the universe [27–30], and baryogenesis and leptogenesis [31, 32] and recently considered in context to non-standard cosmology with axion-driven kination [33–37].¹

In order to describe the scalar field as ALPs their coupling to the SM particles is suppressed by inverse powers of the $U(1)$ symmetry breaking energy scale f_ϕ (also known as the ALP decay constant). This energy scale is usually identified as the vacuum expectation value (VEV) of the SM-singlet complex scalar field Φ , i.e. $\langle \Phi \rangle = f_\phi/\sqrt{2}$, quite larger the electroweak scale $v_{\text{ew}} \simeq 246.2$ GeV in order to evade current experimental and observational limits [12, 17]. The Φ -field can be expressed as:

$$\Phi(x) = \frac{1}{\sqrt{2}} [f_\phi + \sigma(x)] e^{i\phi(x)/f_\phi}. \quad (1)$$

Modulus ϕ of the Φ -field receives a large mass term $m_\phi \sim f_\phi$, and the angular part a becomes the pNGB that acquires a much smaller mass m_a from an explicit low energy $U(1)$ -breaking non-perturbative effects. Therefore, as usually done for any effective-field-theory (EFT) purposes for the low-energy phenomenology of ALPs, the heavier modulus part ϕ can be safely integrated out, and we are left with only independent parameters as the mass of the ALP m and the decay constant f_ϕ . In presence of a dark sector with matter content with at least two fermions, let us call them up-type fermion and down-type fermions², the axion potential does not show the pure cosine behavior but instead slightly modified as we will show in Eqn. (3) [18, 44]. Most of the early works considering axion or ALP as the curvaton considered the radial part of the ALP field or small field regimes of the phase part as the curvaton and studied the generation of primordial density fluctuations as well

¹ Recently, a minimal extension involving SM supplemented with heavy neutrinos and a complex scale whose phase is the axion and the real part generates heavy neutrino masses have been proposed [38–43].

² In pure QCD scenario, this corresponds to up and down type quarks in QCD which couples to the axion, however in our case we will consider generic dark sector and consider an ALP scenario with two dark fermions that couple to it with masses m_u and m_d respectively.

as generation of Primordial Blackholes and secondary Gravitational Waves [45–51]. Very recently in Ref. [53] the non-perturbatively generated cosine part of axion was considered to be the curvaton and investigated the parameter range where the axion may source the correct density perturbations as well as predictions in non-Gaussianity signals. In this paper we will study such an ALP coupled to two dark fermions with masses m_u and m_d in early universe. Particularly, we will consider the ALP as a spectator field during inflation (with sub-dominant energy density compared to the inflaton) and then starts to oscillate and sources density perturbation acting as the curvaton. What we will see is that various combinations of m_u and m_d masses that the ALP couples to we actually we are able to achieve limits behave like quadratic potentials (like the vanilla curvaton) on one hand and cosine potential on the other hand. The results of the respective curvaton scenarios are thus obtained there-in in the same ALP model but due to various choices of the matter content and confining dynamics that couples to the ALP. This will result in detectable predictions in the power spectrum, bi-spectrum and tri-spectrum in CMB.

The paper is organized as follows: in section II, we give a brief overview of the ALP model, in sections III and IV we study ALP as spectator field generating primordial curvature perturbations later on after inflation ends, and also discuss non-Gaussianities. In section V, we show the results of our investigation and we end in section VI with a generalized discussion and the salient features of the ALP as the curvaton that have been manifest.

II. THE AXION SETUP

We consider a pseudo-Nambu goldstone boson (PNGB) of some global U(1) symmetry that is spontaneously broken at an energy scale f_ϕ ; we refer to this field as the axion and f_ϕ the axion decay constant. We also assume the U(1) to be explicitly broken due to the axion being coupled to a new gauge force (not QCD) that becomes strong at low energies, yielding a periodic axion potential [18, 44]. Considering the periodicity to be governed by f_ϕ , we write the axion Lagrangian as

$$\mathcal{L} = -\frac{1}{2}\partial_\mu\phi\partial^\mu\phi - V(\phi) \quad (2)$$

where the behavior of axion potential $V(\phi)$ can be written as,

$$V(\phi) = m_\pi^2 f_\pi^2 \left[1 - \sqrt{1 - \frac{4m_u m_d}{(m_u + m_d)^2} \sin^2 \left(\frac{\phi}{2f_\phi} \right)} \right] \quad (3)$$

where, m_u and m_d are masses of two light quarks, m_π and f_π are the mass and the decay constant of a "dark" pion, and f_ϕ is a constant.

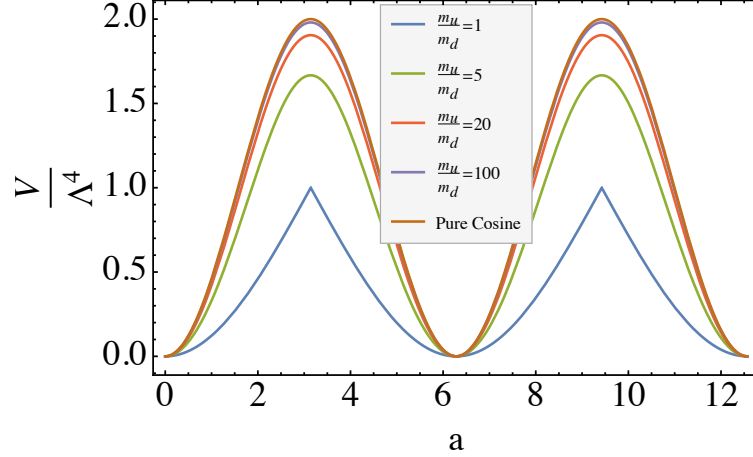


FIG. 1: Plot of $V(a)$ versus a (in arbitrary units) for various limits of m_u and m_d .

The potential (3) depends on the ratio $\frac{m_u}{m_d}$ and in two extreme limits behaves as,

$$V(\phi) = \Lambda^4 \frac{m_d}{m_u} \left[1 - \cos \left(\frac{\phi}{f_\phi} \right) \right] \text{ for } m_u \gg m_d \quad (4)$$

$$V(\phi) = \Lambda^4 \left[1 - \cos \left(\frac{\phi}{2f_\phi} \right) \right] \text{ for } m_u = m_d \quad (5)$$

From Fig 1 we can see that $m_u = m_d$ limit behaves very similar to as vanilla curvaton scenario (since below the cusp $V''(\phi)$ is always positive) and when $m_u \gg m_d$ it behaves as cosine like scenario. Here we have introduced the parameter and set it to $\Lambda^4 = m_\pi^2 f_\pi^2 = m^2 f_\phi^2$.

The zero-temperature axion mass is given by ³

$$m_0 = m = \frac{m_u m_d}{m_u + m_d} \frac{\Lambda^2}{f_\phi}. \quad (7)$$

Without loss of generality we may take the axion to lie within the range $-\pi \leq a \leq \pi$ with $a = \frac{\phi}{f_\phi}$.

III. ALP AS THE CURVATON: COSMOLOGICAL EVOLUTION

The vacuum expectation value (VEV) of the curvaton during inflation is always considered to be a free parameter at the classical level here. Nonetheless, in a long-lived inflationary universe, the long wavelength modes of the quantum fluctuation of a light scalar field may become important, because its Compton wavelength is large compared to the size of the Hubble horizon during inflation. From Ref. [60], we know the vacuum expectation value of the square of such a light scalar field curvaton of mass m_c with potential $V(\sigma_c) = \frac{1}{2}m_c^2\sigma_c^2$ is given by

$$\langle \sigma_c^2 \rangle = \frac{3H_*^4}{8\pi^2 m_c^2}, \quad (8)$$

where H_* is the Hubble parameter during inflation. So the vacuum expectation value of σ_c can be estimated as

$$\sigma_{c*} = \sqrt{\langle \sigma_c^2 \rangle} = \sqrt{\frac{3}{8\pi^2} \frac{H_*^2}{m_c}}. \quad (9)$$

Thus for a curvaton field with quadratic potential, its typical vacuum expectation value is given by H_*^2/m and its energy density is roughly given by H_*^4 . This means that larger the Hubble parameter during inflation, larger the energy density of curvaton. However, the energy density of axion-type curvaton (as in Eqn. (2)) is bounded by $m^2 f^2$ from above. If $mf \gg H_*^2$, σ_{c*} can be estimated as H_*^2/m . On the other hand, $\sigma_{c*} \sim f$ if $mf \leq H_*^2$. Since

³ Usually, below some strong coupling scale Λ ($< f_\phi$), we consider the axion mass to depend as well on the temperature of the Universe

$$m(T) \simeq \begin{cases} m \left(\frac{\Lambda}{T}\right)^Q & \text{for } T > \Lambda, \\ m & \text{for } T < \Lambda, \end{cases} \quad (6)$$

with a positive power Q usually of order unity, as understood via non-perturbative estimations in the strongly coupled regimes. As we are only interested in the $T < \Lambda$ regimes we consider no dependence on T .

it is difficult to get analytic results for the axion-type curvaton model if $\sigma_{c*} \sim f$, we will use numerical method to calculate the curvature perturbation in the next section.

Upon analyzing the axion dynamics, we will make a couple of assumptions along the way.

- We first assume the hierarchy of energy scales $T_{\text{inf}} = H_{\text{inf}}/2\pi$.

$$T_{\text{inf}} < \Lambda < f_\phi. \quad (10)$$

During inflation the U(1) is already broken.

- Then we assume $m^2 \ll H_{\text{inf}}^2$, and that f_ϕ is smaller than the reduced Planck scale $M_{\text{Pl}} = (8\pi G)^{-1/2}$, then $\Lambda^4 \ll M_{\text{Pl}}^2 H_{\text{inf}}^2$, i.e., the energy density of the axion is tiny compared to the total density of the universe and thus the axion serves as a spectator field.
- We assume axion rolling is classical and it rolls slowly and satisfies,

$$3H_{\text{inf}}\dot{\phi} \simeq -\frac{dV(\phi)}{d\phi}. \quad (11)$$

For cosine like potential choice $V(a) = \Lambda^4(1 - \cos a)$ integrating this by ignoring any time dependence of the Hubble rate [53] yields

$$\tan\left(\frac{a_{\text{end}}}{2}\right) \simeq \tan\left(\frac{a_1}{2}\right) \cdot e^{\left(-\frac{m^2}{3H_{\text{inf}}^2}\mathcal{N}_1\right)}, \quad (12)$$

with the identification, $m^2 = \frac{\Lambda^4}{f_\phi^2}$. Here a_{end} is the field value when inflation ends, and \mathcal{N}_1 is the number of e -folds since the time when the axion takes a value a_1 until the end of inflation.

Denoting the axion decay rate as Γ_a^4 , if $\Gamma_a < (>) H_{\text{dom}}$, then the axion would decay after (before) dominating the universe. Supposing that the axion decays suddenly when $H = \Gamma_a$ (we denote quantities at this time by the subscript “dec”), one finds a relation:

$$3M_{\text{Pl}}^2\Gamma_a^2 = \rho_{r,\text{osc}}\left(\frac{a_{\text{osc}}}{a_{\text{dec}}}\right)^4 + \rho_{a,\text{osc}}\left(\frac{a_{\text{osc}}}{a_{\text{dec}}}\right)^3. \quad (13)$$

The terms in the right hand side correspond to the radiation and axion densities right before the decay, and we write their ratio as $R \equiv (\rho_a/\rho_r)_{\text{dec}}$ for later convenience.

⁴ This decay width Γ_a is generated due to axion couplings to fermions or gauge bosons or to other scalars, however we do not discuss the microscopic details of the ALP model and instead resort to the decay as a phenomenological parameter. For BSM model details for such Γ_a the reader is referred to Ref. [18].

IV. CURVATURE PERTURBATION AND NON-GAUSSIANITIES

A. Analytical Solutions

Converting isocurvature perturbations to adiabatic ones, the conversion is completed when the axion decays. Using the $\delta\mathcal{N}$ formalism [51], we compute the axion-induced curvature perturbation as the fluctuation in the number of e -folds \mathcal{N} between an initial flat slice during inflation when a comoving wave number k of interest exists the horizon ($k = aH$), and a final uniform-density slice where $H = \Gamma_a$. Power spectrum, and Non-Gaussianities (local bi-spectrum and tri-spectrum)

$$P_\zeta(k) \simeq (\partial\mathcal{N}/\partial a_k)^2 (H_k/2\pi f_\phi)^2 \quad (14)$$

$$f_{\text{NL}} \simeq (5/6)(\partial^2\mathcal{N}/\partial a_k^2)(\partial\mathcal{N}/\partial a_k)^{-2} \quad (15)$$

$$g_{\text{NL}} \simeq (25/54)(\partial^3\mathcal{N}/\partial a_k^3)(\partial\mathcal{N}/\partial a_k)^{-3} \quad (16)$$

Now if we consider a cosine potential for the axion field $V(a) = \Lambda^4 [1 - \cos(a)]$ the above power spectrum and bispectrum can be written as [45, 53]:

$$P_\zeta(k) \simeq \left(\frac{R}{3R+4} \frac{1 + \cos a_{\text{end}}}{\sin a_k} \frac{H_k}{2\pi f_\phi} \right)^2 \quad (17)$$

$$f_{\text{NL}} \simeq \frac{5}{6} \left\{ \frac{4}{R} + \frac{4}{3R+4} - \left(3 + \frac{4}{R} \right) \frac{1 - \cos a_{\text{end}} + \cos a_k}{1 + \cos a_{\text{end}}} \right\},$$

and the tri-spectrum can be written as,

$$g_{\text{NL}} \simeq \frac{25}{54} \left\{ -4(1+R) \left(\frac{4}{R^2} + \frac{12}{(3R+4)^2} \right) + 2 \left(\frac{4}{R} + \frac{4}{(3R+4)} \right)^2 \right. \\ \left. - 3 \left(3 + \frac{4}{R} \right) \left(\frac{4}{R} + \frac{4}{3R+4} \right) \frac{1 - \cos a_{\text{end}} + \cos a_k}{1 + \cos a_{\text{end}}} + \left(3 + \frac{4}{R} \right)^2 \right. \\ \left. \left[\left(\frac{1 - \cos a_{\text{end}} + \cos a_k}{1 + \cos a_{\text{end}}} \right)^2 + \frac{\cos^2 a_{\text{end}} + \cos a_k - \cos a_k \cos a_{\text{end}}}{(1 + \cos a_{\text{end}})^2} \right] \right\} \quad (18)$$

The spectral index of the power spectrum $n_s - 1 = d \ln P_\zeta / d \ln k$ can be computed using $d \ln k \simeq H_k dt$ and the slow-roll approximation during inflation as

$$n_s - 1 \simeq \frac{2}{3} \frac{V''(\phi)}{H_k^2} \cos a_k + 2 \frac{\dot{H}_k}{H_k^2}. \quad (19)$$

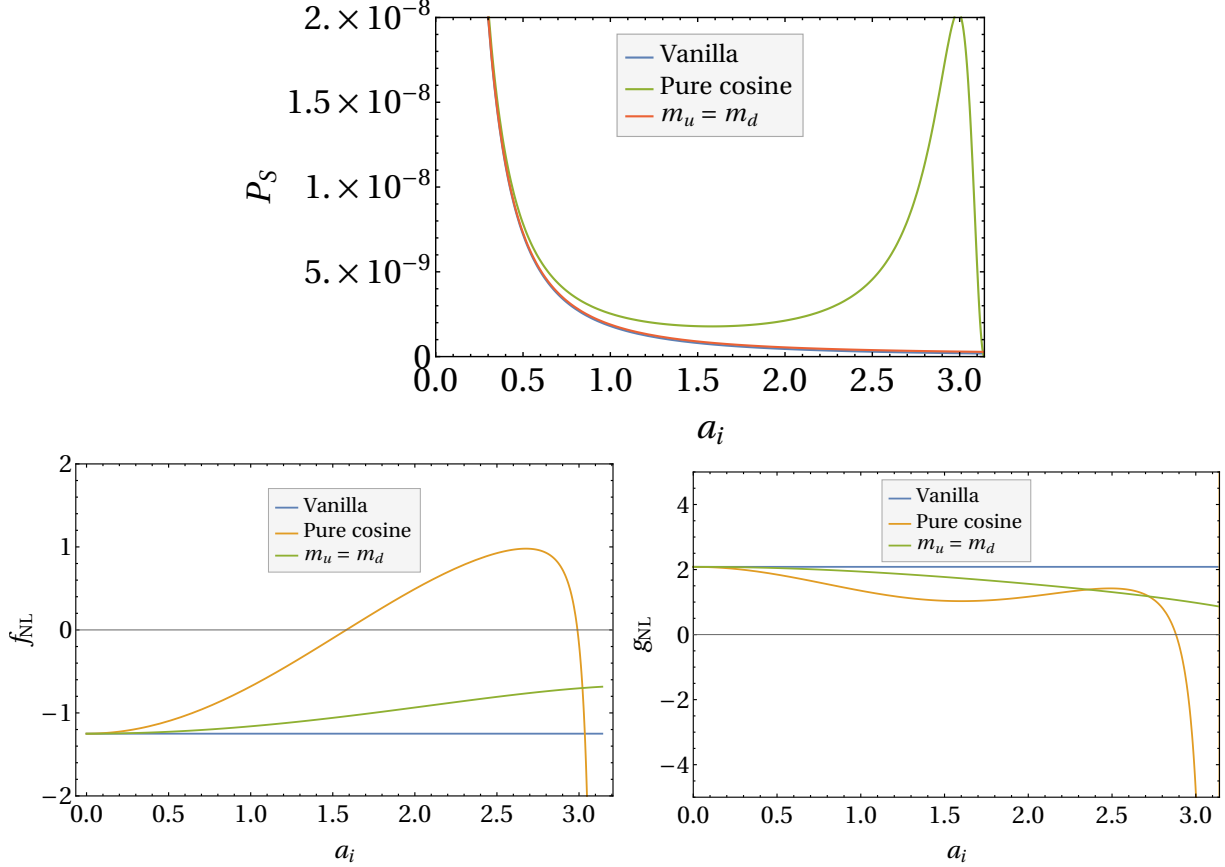


FIG. 2: Analytical estimates for the scalar power spectrum, bi-spectrum and tri-spectrum. It can be noted that for $m_u = m_d$ limit the power spectrum behaves like vanilla scenario. The correlation functions for cosine potential has distinct nature compared to the vanilla case and $m_u = m_d$ case as in this case the correlation functions depend non-trivially on a_i . Also for $m_u = m_d$ case the bispectrum and trispectrum both depend on a_i unlike the vanilla scenario. Parameter choice for all three plots are $H_{\text{inf}} = 10^{-5} M_{\text{Pl}}$, $f_\phi = 2500 H_{\text{inf}}$ & $\Lambda = 30 H_{\text{inf}}$.

We would work in $R \rightarrow \infty$ and it is easy to see that when $a \rightarrow 0$ this expressions produce the correlation functions of vanilla axion scenario. In general the last term in (17) is the first slow roll parameter and is tightly constrained from tensor-to-scalar ratio or equivalently from the single field consistency relation. But in the case of curvaton scenario as the curvaton field is sourcing the perturbations the last term in (17) can be larger than the Planck constraint and can be estimated as 0.02 [52].

One important thing to note here is that the nature of potential (3) becomes $V = \Lambda^4(1 - \cos(a/2))$ in $m_u = m_d$ limit (see (5)) and from here we can easily estimate the

power spectrum for Eqn. (3) potential in $m_u = m_d$ limit as,

$$P_\zeta(k) \simeq \left(\frac{R}{3R+4} \frac{1 + \cos a_{\text{end}}}{\sin a_k} \frac{H_k}{2\pi(2f_\phi)} \right)^2 \quad \text{for } m_u = m_d. \quad (20)$$

and the higher order correlation functions for this scenario can be written as,

$$f_{\text{NL}} \simeq \frac{5}{6} \left\{ \frac{4}{R} + \frac{4}{3R+4} - \left(3 + \frac{4}{R} \right) \frac{1 - \cos \frac{a_{\text{end}}}{2} + \cos \frac{a_k}{2}}{1 + \cos \frac{a_{\text{end}}}{2}} \right\} \quad (21)$$

$$g_{\text{NL}} \simeq \frac{25}{54} \left\{ -4(1+R) \left(\frac{4}{R^2} + \frac{12}{(3R+4)^2} \right) + 2 \left(\frac{4}{R} + \frac{4}{(3R+4)} \right)^2 \right. \\ \left. - 3 \left(3 + \frac{4}{R} \right) \left(\frac{4}{R} + \frac{4}{3R+4} \right) \frac{1 - \cos \frac{a_{\text{end}}}{2} + \cos \frac{a_k}{2}}{1 + \cos \frac{a_{\text{end}}}{2}} + \left(3 + \frac{4}{R} \right)^2 \right. \\ \left. \left[\left(\frac{1 - \cos \frac{a_{\text{end}}}{2} + \cos \frac{a_k}{2}}{1 + \cos \frac{a_{\text{end}}}{2}} \right)^2 + \frac{\cos^2 \frac{a_{\text{end}}}{2} + \cos \frac{a_k}{2} - \cos \frac{a_k}{2} \cos \frac{a_{\text{end}}}{2}}{(1 + \cos \frac{a_{\text{end}}}{2})^2} \right] \right\} \quad (22)$$

From the analytical expressions for correlation functions as shown in Fig 2 and we can see that the nature of power spectrum for vanilla axion case and $m_u = m_d$ limit of potential (3) are almost identical as it is evident from the nature of (3) which suggests that as m_u becomes equal to m_d the potential behaves more like a vanilla axion scenario (see fig 1). The nature of (3) also suggests that as m_u becomes larger than m_d the potential starts to behave more as a pure cosine kind of axion potential and we can expect that for $m_u \gg m_d$ limit the power spectrum will behave closely as Eqn. (17). The power spectrum in the pure cosine case has a distinct behavior compared to the vanilla case and $m_u = m_d$ case. The bispectrum for pure cosine limit exhibits positive and negative f_{NL} values depending on the value of a_i . The trispectrum becomes negative at large a_i value. It is also important to note here that the nature of bispectrum and trispectrum for $m_u = m_d$ case is completely different than vanilla scenario and these higher order correlation functions have a_i dependence as opposed to vanilla case where these higher order correlation functions are perfectly constant. This is expected as for $m_u = m_d$ case as the potential does not exactly boil down to vanilla scenario, but the power spectrum can not distinguish between these natures while bispectrum and trispectrum can. Also, the bispectrum remains negative for all a_i values and trispectrum remains positive for all a_i values for both the cases.

In Fig. 3 we have plotted the power spectrum, bispectrum and trispectrum for $m_u = m_d$, pure axion and vanilla scenarios for $f_\phi = 2100H_{\text{inf}}$ and $\Lambda = 20H_{\text{inf}}$. Comparing with Fig. 2

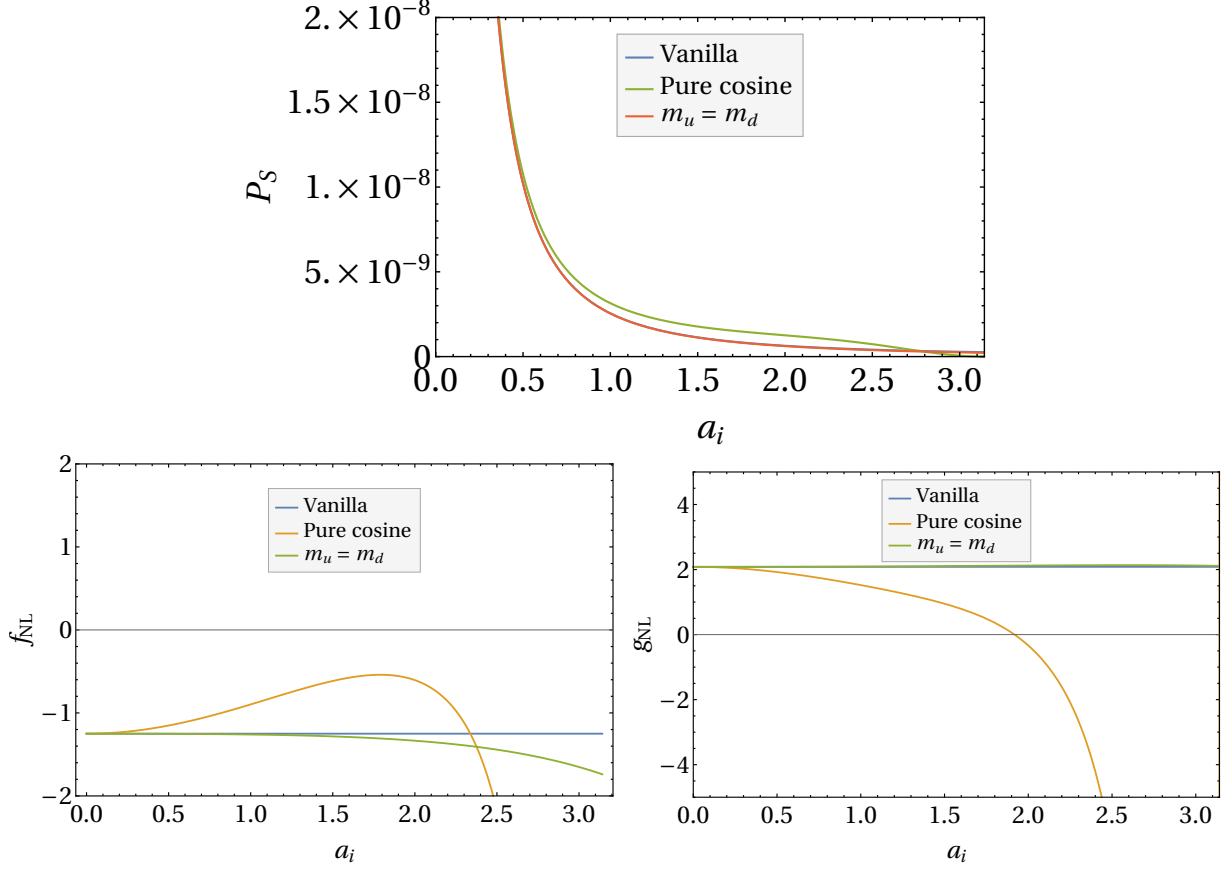


FIG. 3: Analytical estimates for the scalar power spectrum, bi-spectrum and tri-spectrum for $H_{\text{inf}} = 10^{-5} M_{\text{Pl}}$, $f_\phi = 2100 H_{\text{inf}}$ & $\Lambda = 20 H_{\text{inf}}$.

we can see that the behavior of the correlation functions completely changes for this choice of the parameters of the model. Here the power spectrum for pure axion case mostly follows the vanilla-like behavior with a larger amplitude for large a_i values. But the bispectrum has only negative values for all a_i values even for the pure axion case. Also, the trispectrum becomes negative for a smaller a_i value than the previous case for the pure axion case and while it remains constant for both vanilla and $m_u = m_d$ cases.

Though the correlation functions for $m_u = m_d$ and pure axion case can be derived exactly analytically it becomes complicated to evaluate the correlation function in different limits of m_u and m_d analytically, so in the next section we will discuss the numerical evaluation of the correlation functions.

B. Numerical Solution

In this section, we describe the detailed analysis of the results obtained. So far we have introduced the analytical expressions for the scalar power spectrum, bi-spectrum and tri-spectrum. In order to complete our analysis we would focus on numerical solutions also. The evolution of the axion field during inflation will be governed by [54, 55]:

$$3H_{inf}\dot{a} \simeq -\frac{dV(a)}{da}. \quad (23)$$

For the post-inflationary period we have solved the full set of Friedmann equations along with Klein-Gordon equation for axion field a ,

$$\begin{aligned} H_{inf}^2 &= \frac{1}{3M_{Pl}^2} (\rho_r + \rho_a) \\ \dot{\rho}_r + 4H\rho_r &= 0 \\ \rho_a &= \frac{1}{2}\dot{a}^2 + V(a) \\ \ddot{a} + 3H\dot{a} + \frac{dV(a)}{da} &= 0 \end{aligned} \quad (24)$$

Here ρ_r and ρ_a are energy densities of radiation and axion field respectively. These four set of equations can be converted into two set of coupled equations with redefined variables, $x = mt$ as [55],

$$\begin{aligned} \frac{dN}{dx} &= \left[\alpha e^{-4N} + \frac{f_\phi^2}{3M_{Pl}^2} \left\{ \frac{1}{2} \left(\frac{da}{dx} \right)^2 + V(a) \right\} \right]^{\frac{1}{2}} \\ \frac{d^2a}{dx^2} &= -3 \frac{dN}{dx} \frac{da}{dx} - \frac{dV(a)}{da} \end{aligned} \quad (25)$$

Here, $\alpha = \rho_{r,0}/(3m^2M_{Pl}^2)$ and can be considered $\mathcal{O}(1)$ because at the end of inflation the energy density of radiation was dominant and so at $H_{inf} = m$, $\rho_{r,0} = 3m^2M_{Pl}^2$. The numerical integration would be done from the time when the axion starts to oscillate at $H_{inf} = m$ i.e $x = 1$ until the axion field decays at $H_{inf} = \Gamma_a$ i.e $x = \frac{m}{\Gamma_a}$. One important point to notice here is that in the equation of motion of the axion field we do not consider the effect of the decay width Γ_a as we are working in $R \rightarrow \infty$ and as a result Γ_a is very small compared to the axion mass and here we are considering $\Gamma_a/m \sim 10^{-16}$.

V. MATCHING WITH PLANCK OBSERVATIONS

In this section, we compute the power spectrum, bi-spectrum and tri-spectrum numerically and normalize with the Planck data.

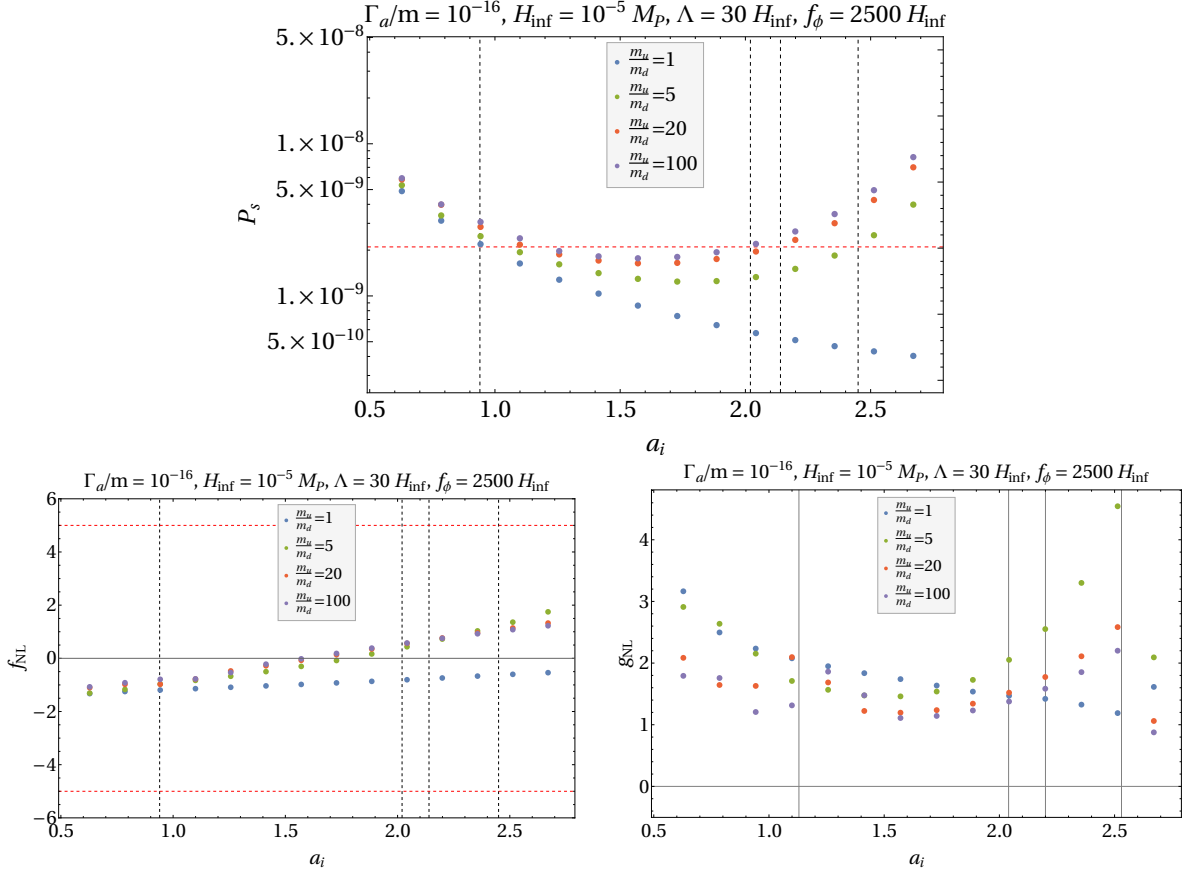


FIG. 4: Plots of scalar power spectrum P_s , scalar bi-spectrum f_{NL} and scalar tri-spectrum g_{NL} versus a_i . We show the dependence of the spectra on various combinations of m_u and m_d masses for the parameters $\frac{\Gamma_a}{m} = 10^{-16}$, $H_{\text{inf}} = 10^{-5} M_{\text{Pl}}$, $f_\phi = 2500 H_{\text{inf}}$ & $\Lambda = 30 H_{\text{inf}}$. The horizontal red lines show Planck's bound on the respective observables. The vertical dotted lines describe the value of a_i where the Planck normalization for the scalar power spectrum is satisfied for different m_u and m_d limits. Here we only include the a_i range where we can trust our numerical results.

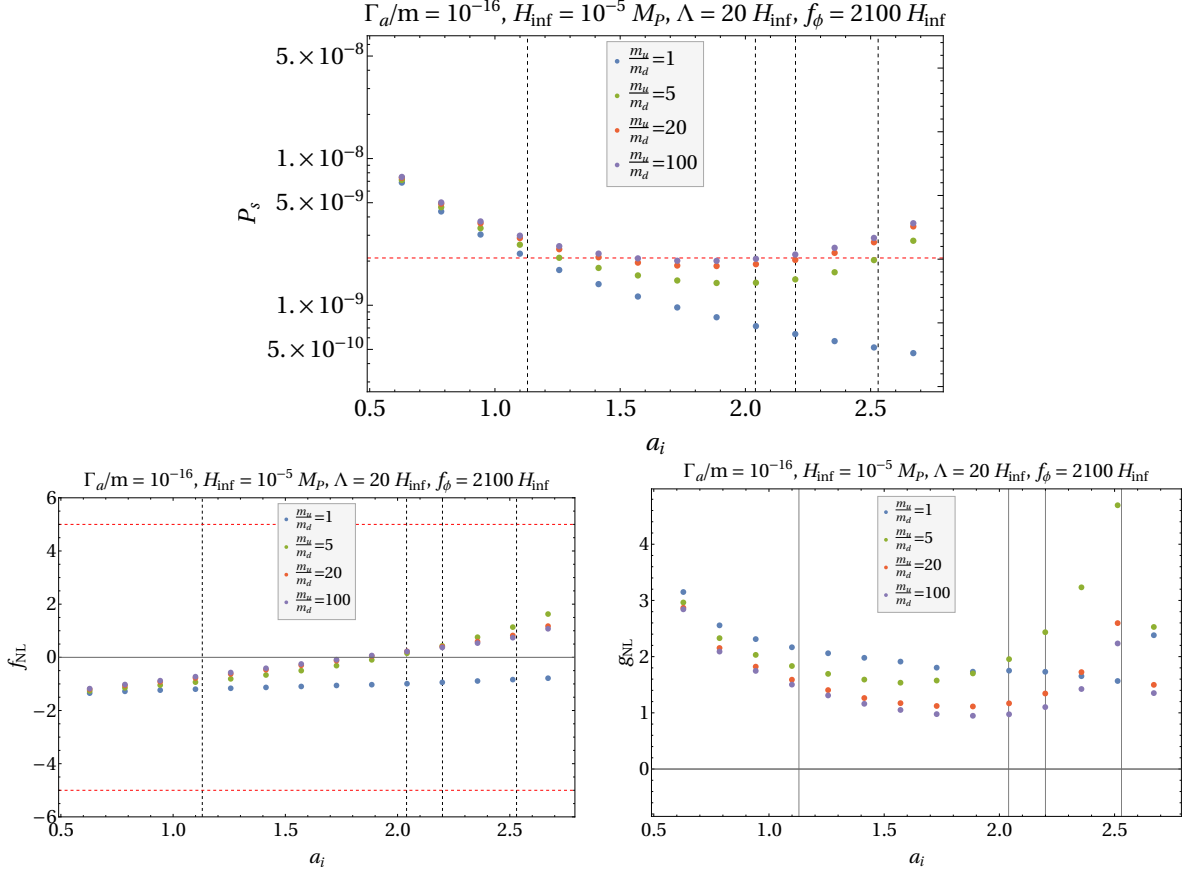


FIG. 5: Plots of scalar power spectrum P_s , scalar bi-spectrum f_{NL} and scalar tri-spectrum g_{NL} versus a_i . We show the dependence of the spectra on various combinations of m_u and m_d masses for the parameters $\frac{\Gamma_a}{m} = 10^{-16}$, $H_{\text{inf}} = 10^{-5} M_{\text{Pl}}$, $f_\phi = 2100 H_{\text{inf}}$ & $\Lambda = 20 H_{\text{inf}}$. The horizontal red lines show Planck's bound on the respective observables. The vertical dotted lines describe the value of a_i where the Planck normalization for the scalar power spectrum is satisfied for different m_u and m_d limits. Here we only include the a_i range where we can trust our numerical results.

In Figs. 4 and 5 we have analyzed the power spectrum, bi-spectrum and tri-spectrum for the parameter choice: $\Gamma_a/m = 10^{-16}$, $H_{\text{inf}} = 10^{-5} M_{\text{Pl}}$, with $\Lambda = 30 H_{\text{inf}}$, $f_\phi = 2500 H_{\text{inf}}$ and $\Lambda = 20 H_{\text{inf}}$, $f_\phi = 2100 H_{\text{inf}}$ respectively. We have compared them with recent Planck constraints⁵. If we compare the behavior of the correlators estimated numerically in Fig. 4 with the analytical one in Fig. 2 where $\Lambda = 30 H_{\text{inf}}$, $f_\phi = 2500 H_{\text{inf}}$ we can see that the nature of the numerical estimation closely follows the analytical behavior except for large a_i range. This is because the dependence of the mass-to-Hubble ratio is always taken to be

⁵ We have included only the range of a_i in Fig. 4 where the numerical result can be trusted.

constant and this approximation can break down for large a_i limit [53]. But if we compare the numerical estimation of Fig. 5 with Fig. 3 where $\Lambda = 20H_{\text{inf}}$, $f_\phi = 2100H_{\text{inf}}$ we can see that there is a huge disagreement between the analytical and numerical estimation. In the former, we can see that the power spectrum for pure cosine case closely follows the vanilla scenario but in the numerical estimation for $m_u/m_d = 100$ which closely behaves like a cosine potential, we can see that the power spectrum behaves differently compared to the vanilla case and also compared to the $m_u/m_d = 1$ case which closely resembles the vanilla scenario. Also in the $m_u/m_d = 100$ limit with numerical estimation, we can see that f_{NL} can have both positive and negative values depending on a_i but in the analytical case, we have seen that with this parameter choice f_{NL} was always negative for pure axion case. This discrepancy arises because in the analytical estimation, we have started with Eqn. (13) where we have considered the energy of the axion redshifts as a^{-3} . With this consideration, we have performed derivatives of the number of e-folds with respect to the field value to compute the correlation functions. But this approximation breaks down if the potential cannot be approximated as $m^2 a^2$ type. As the axion potential of Eqn. (3) is different from $m^2 a^2$ type, the analytical and numerical results do not match for most of the parameter space under consideration.

As for the numerical behavior of the correlators, the first thing to notice here is that the scalar power spectrum matches the Planck bound at different a_i values for different m_u/m_d choices. With $f_\phi = 2500H_{\text{inf}}$ and $\Lambda = 30H_{\text{inf}}$ when $m_u/m_d = 1$ the power spectrum is normalized at $a_i \sim 0.94$, when $m_u/m_d = 5$ at $a_i \sim 2.45$, at $a_i \sim 2.14$ for $m_u/m_d = 20$ and $a_i \sim 2.02$ when $m_u/m_d = 100$. This behavior can be explained from Fig 1 where we have seen that when $m_u = m_d$ the potential actually behaves very close to as a quadratic potential and the nature of the power spectrum is very close to the vanilla case as can also be seen in Fig 2. Now as m_u starts to get larger than m_d the potential starts to behave more as a cosine kind of potential and the nature of the power spectrum for three $m_u \neq m_d$ cases discussed above starts to behave as the power spectrum in the case of cosine potential. Although one important thing to note here is that the Planck normalization of the power spectrum for these three cases are met at three different values of a_i . For same choice of Γ_a/m , H_{inf} , Λ and f_ϕ the power spectrum matches the Planck normalization at largest a_i value for $m_u/m_d = 5$ case and smallest a_i value for $m_u/m_d = 100$ case. So as m_u gets larger than m_d i.e as the potential starts to behave more and more like a cosine potential and

smaller value of a_i satisfies Planck normalization.

Now if we focus on the bispectrum we can see that the $m_u = m_d$ case has very small a_i dependence but certainly not constant and $f_{NL} \sim -1.15$ consistent with Planck normalization of the power spectrum. Now the bispectrum in the vanilla case is constant $f_{NL} \sim -1.25$; so even if the power spectrum for $m_u = m_d$ case and vanilla scenario are very similar in nature there is a clear distinction in the behavior of bispectrum. For the three $m_u \neq m_d$ cases we see that the largest $f_{NL} \sim 1.19$ one can get from $m_u/m_d = 5$ and the value for f_{NL} decreases as m_u gets larger and larger than m_d with $f_{NL} \sim 0.69$ for $m_u/m_d = 20$ and $f_{NL} \sim 0.55$ for $m_u/m_d = 100$ cases. So in general we can see that as m_u/m_d becomes larger i.e., as the potential becomes more like a cosine potential than the vanilla kind of nature the amplitude of bispectrum decreases. The nature of the trispectrum follows the behavior of the bispectrum very closely. Again $m_u/m_d = 1$ case have a a_i dependence which is not observed in the vanilla case and the amplitude of the trispectrum decreases with the increasing value of m_u/m_d . If we choose $f_\phi = 2100H_{\text{inf}}$ and $\Lambda = 20H_{\text{inf}}$ the power spectrum gets normalized at $a_i \sim 0.94$ for $m_u/m_d = 1$, at $a_i \sim 2.52$ for $m_u/m_d = 5$, $a_i \sim 2.19$ for $m_u/m_d = 20$ and $a_i \sim 2.04$ for $m_u/m_d = 100$. So the normalization shifts towards the right in a_i values for this parameter choice compared to the previous case.

One of the most important aspects of our model is that it produces different aspects of ALP behavior in different m_u/m_d limits and upcoming more precise data can help us put bound on the m_u/m_d limit and hence pinpoint the axion behavior. In our analysis, we have seen that the power spectrum can be the main distinguishing factor between the different limits of m_u/m_d as it satisfies the Planck bound in different a_i limits. Also, the estimation of bi-spectrum and tri-spectrum can be a crucial factor as we have seen that the different cases can produce very different f_{NL} and g_{NL} values. Although the scope of exploring the details of the parameter space involving f_ϕ and Λ is beyond the scope of the present manuscript we comment on the implications on the parameter space. The variations of f_ϕ and Λ will shift the Planck normalization a_i values in Fig. 4. For certain choices of f_ϕ and Λ we will not be able to satisfy the normalization for any a_i values. However, the important point to note is that in the case where our normalization is satisfied at small a_i values, the results will be similar to the vanilla curvaton which means negative f_{NL} . On the other hand for larger a_i normalization, we should expect positive f_{NL} , g_{NL} is however always positive irrespective of these choices.

VI. CONCLUSIONS AND DISCUSSION

We investigated and showed that an axion like particle with the precise axion potential, coupled to a new confining dark sector (with matter content involving dark fermions) can generate the primordial density perturbation of our universe even if the same from the inflaton is not sufficient. The axion decay constant f_ϕ , the scale of confinement Λ of the dark sector and the masses m_u and m_d of the dark fermions that couple to the ALP are determined by observations in terms of the inflation scale H_{inf} , which, in the minimal model, manifests a temporal de-confinement of the gauge group after inflation. Our investigations lead to the following results:

- For the pure cosine ALP potential we provide analytical estimates for the power spectrum, bi-spectrum and tri-spectrum as given in Eqns. (17) & (18) and shown in Fig. 2 for the parameter values $f_\phi = 2500H_{\text{inf}}$ and $\Lambda = 30H_{\text{inf}}$ when $m_u/m_d = 1$. Particularly the tri-spectrum for ALP is derived for the first-time in the literature according to our knowledge.
- We studied the scenario for various combinations of m_u and m_d values which generates a non-perturbative potential which is not of purely cosine form (see Eqn. (3)). We have derived the analytical expressions for the power spectrum and higher order correlation functions (see Eqns. (20), (21) and (22)) for $m_u/m_d = 1$ limit. In this scenario we have found that the power spectrum behaves very similarly to the vanilla curvaton (with quadratic potential) scenario. But when we compute the bispectrum and trispectrum we can clearly see that these higher order correlation functions actually have an a_i dependence when for vanilla curvaton case these correlation functions are constants. For other limits of m_u and m_d we have done numerical estimations and we have observed that their power spectrum gets normalized (due to Planck observation) at different values of a_i and as a result the amplitude of bispectrum and trispectrum are different for different cases (see Fig. 4).
- We observed that the value of f_{NL} and g_{NL} are dependent on the ratio of m_u and m_d . Apart from the $m_u = m_d$ case we have seen that the value of f_{NL} is positive for all the other cases and g_{NL} is always positive irrespective of the ratio between m_u and m_d . From Fig. 4 it is evident that the value of f_{NL} increases as the ratio between m_u

and m_d becomes smaller i.e as the behavior of the potential deviates from pure cosine one towards the vanilla one the f_{NL} increases. The same conclusion can be drawn for the nature of g_{NL} also.

- The results of our curvaton analysis in the limit $m_u = m_d$ resembles that of the vanilla curvaton (quadratic potential) scenario while in the limit $m_u \gg m_d$ resembles axion (pure cosine) potential, that is without having any corrections from new dark sector fermions.

These interesting features along with non-gaussianities f_{NL} and g_{NL} can be further verified observationally by using, for instance, ultracompact minihalos and generation of Primordial Blackholes [49] and secondary Gravitational Waves, including the recently detected signals in NanoGrav, as shown in Refs. [50]; such a study is beyond the current draft and will taken up in later publication. Thus we dare to imagine particle physics models such as ALP which is otherwise motivated from the Strong CP problem may also be responsible for large scale structure as we see today, thereby connecting the small scale nature of quantum particle theory of fundamental interactions to the observation of very large scale structures that we see in the universe.

Acknowledgement

Authors thank Alessio Notari for collaborating on early stages of the project and Dario Bettoni, Maximilian Berbig and Keisuke Inomata for careful reading of the manuscript and suggestions.

-
- [1] D. H. Lyth and A. R. Liddle, *The primordial density perturbation*, Cambridge University Press, 2009.
- [2] K. Dimopoulos, M. Karčiauskas, D. H. Lyth, Y. Rodriguez, JCAP **0905**, 013 (2009).
- [3] D. H. Lyth and D. Wands, Phys. Lett. B **524**, 5 (2002); D. H. Lyth, C. Ungarelli and D. Wands, Phys. Rev. D **67**, 023503 (2003). (see also K. Enqvist and M. S. Sloth, Nucl. Phys. B **626** (2002) 395).

- [4] A. Linde and V. Mukhanov, Phys. Rev. D **56**, R535 (1997); T. Moroi and T. Takahashi, Phys. Lett. B **522**, 215 (2001). Erratum-ibid B **539**, 303 (2002).
- [5] R. D. Peccei and H. R. Quinn, Phys. Rev. Lett. **38**, 1440-1443 (1977)
doi:10.1103/PhysRevLett.38.1440
- [6] R. D. Peccei and H. R. Quinn, Phys. Rev. D **16**, 1791-1797 (1977)
doi:10.1103/PhysRevD.16.1791
- [7] S. Weinberg, Phys. Rev. Lett. **40**, 223-226 (1978) doi:10.1103/PhysRevLett.40.223
- [8] F. Wilczek, Phys. Rev. Lett. **40**, 279-282 (1978) doi:10.1103/PhysRevLett.40.279
- [9] K. Hamaguchi, N. Nagata, K. Yanagi and J. Zheng, Phys. Rev. D **98**, no.10, 103015 (2018)
doi:10.1103/PhysRevD.98.103015 [arXiv:1806.07151 [hep-ph]].
- [10] M. V. Beznogov, E. Rrapaj, D. Page and S. Reddy, Phys. Rev. C **98**, no.3, 035802 (2018)
doi:10.1103/PhysRevC.98.035802 [arXiv:1806.07991 [astro-ph.HE]].
- [11] L. B. Leinson, JCAP **11**, 031 (2019) doi:10.1088/1475-7516/2019/11/031 [arXiv:1909.03941 [hep-ph]].
- [12] J. Jaeckel and A. Ringwald, Ann. Rev. Nucl. Part. Sci. **60**, 405-437 (2010)
doi:10.1146/annurev.nucl.012809.104433 [arXiv:1002.0329 [hep-ph]].
- [13] A. Ringwald, Phys. Dark Univ. **1**, 116-135 (2012) doi:10.1016/j.dark.2012.10.008
[arXiv:1210.5081 [hep-ph]].
- [14] P. Arias, D. Cadamuro, M. Goodsell, J. Jaeckel, J. Redondo and A. Ringwald, JCAP **06**, 013 (2012) doi:10.1088/1475-7516/2012/06/013 [arXiv:1201.5902 [hep-ph]].
- [15] P. W. Graham, I. G. Irastorza, S. K. Lamoreaux, A. Lindner and K. A. van Bibber, Ann. Rev. Nucl. Part. Sci. **65**, 485-514 (2015) doi:10.1146/annurev-nucl-102014-022120
[arXiv:1602.00039 [hep-ex]].
- [16] D. J. E. Marsh, Phys. Rept. **643**, 1-79 (2016) doi:10.1016/j.physrep.2016.06.005
[arXiv:1510.07633 [astro-ph.CO]].
- [17] I. G. Irastorza and J. Redondo, Prog. Part. Nucl. Phys. **102**, 89-159 (2018)
doi:10.1016/j.pnpnp.2018.05.003 [arXiv:1801.08127 [hep-ph]].
- [18] L. Di Luzio, M. Giannotti, E. Nardi and L. Visinelli, Phys. Rept. **870**, 1-117 (2020)
doi:10.1016/j.physrep.2020.06.002 [arXiv:2003.01100 [hep-ph]].
- [19] A. Arvanitaki, S. Dimopoulos, S. Dubovsky, N. Kaloper and J. March-Russell, Phys. Rev. D **81**, 123530 (2010) doi:10.1103/PhysRevD.81.123530 [arXiv:0905.4720 [hep-th]].

- [20] P. W. Graham, D. E. Kaplan and S. Rajendran, *Phys. Rev. Lett.* **115**, no.22, 221801 (2015) doi:10.1103/PhysRevLett.115.221801 [arXiv:1504.07551 [hep-ph]].
- [21] K. Freese, J. A. Frieman and A. V. Olinto, *Phys. Rev. Lett.* **65**, 3233-3236 (1990) doi:10.1103/PhysRevLett.65.3233
- [22] F. C. Adams, J. R. Bond, K. Freese, J. A. Frieman and A. V. Olinto, *Phys. Rev. D* **47**, 426-455 (1993) doi:10.1103/PhysRevD.47.426 [arXiv:hep-ph/9207245 [hep-ph]].
- [23] R. Daido, F. Takahashi and W. Yin, *JCAP* **05**, 044 (2017) doi:10.1088/1475-7516/2017/05/044 [arXiv:1702.03284 [hep-ph]].
- [24] J. Preskill, M. B. Wise and F. Wilczek, *Phys. Lett. B* **120**, 127-132 (1983) doi:10.1016/0370-2693(83)90637-8
- [25] L. F. Abbott and P. Sikivie, *Phys. Lett. B* **120**, 133-136 (1983) doi:10.1016/0370-2693(83)90638-X
- [26] M. Dine and W. Fischler, *Phys. Lett. B* **120**, 137-141 (1983) doi:10.1016/0370-2693(83)90639-1
- [27] P. Jain, *Mod. Phys. Lett. A* **20**, 1763-1766 (2005) doi:10.1142/S0217732305016890 [arXiv:hep-ph/0411279 [hep-ph]].
- [28] J. E. Kim and H. P. Nilles, *JCAP* **05**, 010 (2009) doi:10.1088/1475-7516/2009/05/010 [arXiv:0902.3610 [hep-th]].
- [29] J. E. Kim and H. P. Nilles, *Phys. Lett. B* **730**, 53-58 (2014) doi:10.1016/j.physletb.2014.01.031 [arXiv:1311.0012 [hep-ph]].
- [30] A. Lloyd-Stubbs and J. McDonald, *Phys. Rev. D* **99**, no.2, 023510 (2019) doi:10.1103/PhysRevD.99.023510 [arXiv:1807.00778 [hep-ph]].
- [31] R. Daido, N. Kitajima and F. Takahashi, *JCAP* **07**, 046 (2015) doi:10.1088/1475-7516/2015/07/046 [arXiv:1504.07917 [hep-ph]].
- [32] A. De Simone, T. Kobayashi and S. Liberati, *Phys. Rev. Lett.* **118**, no.13, 131101 (2017) doi:10.1103/PhysRevLett.118.131101 [arXiv:1612.04824 [hep-ph]].
- [33] R. T. Co, L. J. Hall and K. Harigaya, *Phys. Rev. Lett.* **124**, no.25, 251802 (2020) doi:10.1103/PhysRevLett.124.251802 [arXiv:1910.14152 [hep-ph]].
- [34] R. T. Co and K. Harigaya, *Phys. Rev. Lett.* **124**, no.11, 111602 (2020) doi:10.1103/PhysRevLett.124.111602 [arXiv:1910.02080 [hep-ph]].
- [35] R. T. Co, N. Fernandez, A. Ghalsasi, L. J. Hall and K. Harigaya, *JHEP* **03**, 017 (2021) doi:10.1007/JHEP03(2021)017 [arXiv:2006.05687 [hep-ph]].

- [36] K. Harigaya and I. R. Wang, *JHEP* **10**, 022 (2021) [erratum: *JHEP* **12**, 193 (2021)] doi:10.1007/JHEP10(2021)022 [arXiv:2107.09679 [hep-ph]].
- [37] R. T. Co, K. Harigaya, Z. Johnson and A. Pierce, *JHEP* **11**, 210 (2021) doi:10.1007/JHEP11(2021)210 [arXiv:2110.05487 [hep-ph]].
- [38] A. Salvio, *Phys. Lett. B* **743**, 428-434 (2015) doi:10.1016/j.physletb.2015.03.015 [arXiv:1501.03781 [hep-ph]].
- [39] G. Ballesteros, J. Redondo, A. Ringwald and C. Tamarit, *Phys. Rev. Lett.* **118**, no.7, 071802 (2017) doi:10.1103/PhysRevLett.118.071802 [arXiv:1608.05414 [hep-ph]].
- [40] G. Ballesteros, J. Redondo, A. Ringwald and C. Tamarit, *JCAP* **08**, 001 (2017) doi:10.1088/1475-7516/2017/08/001 [arXiv:1610.01639 [hep-ph]].
- [41] Y. Ema, K. Hamaguchi, T. Moroi and K. Nakayama, *JHEP* **01**, 096 (2017) doi:10.1007/JHEP01(2017)096 [arXiv:1612.05492 [hep-ph]].
- [42] A. Salvio, *Phys. Rev. D* **99**, no.1, 015037 (2019) doi:10.1103/PhysRevD.99.015037 [arXiv:1810.00792 [hep-ph]].
- [43] R. S. Gupta, J. Y. Reiness and M. Spannowsky, *Phys. Rev. D* **100**, no.5, 055003 (2019) doi:10.1103/PhysRevD.100.055003 [arXiv:1902.08633 [hep-ph]].
- [44] G. Grilli di Cortona, E. Hardy, J. Pardo Vega and G. Villadoro, *JHEP* **01**, 034 (2016) doi:10.1007/JHEP01(2016)034 [arXiv:1511.02867 [hep-ph]].
- [45] M. Kawasaki, T. Kobayashi and F. Takahashi, *Phys. Rev. D* **84**, 123506 (2011) doi:10.1103/PhysRevD.84.123506 [arXiv:1107.6011 [astro-ph.CO]].
- [46] M. Kawasaki, N. Kitajima and T. T. Yanagida, *Phys. Rev. D* **87**, no.6, 063519 (2013) doi:10.1103/PhysRevD.87.063519 [arXiv:1207.2550 [hep-ph]].
- [47] M. Kawasaki, T. Kobayashi and F. Takahashi, *JCAP* **03**, 016 (2013) doi:10.1088/1475-7516/2013/03/016 [arXiv:1210.6595 [astro-ph.CO]].
- [48] K. Ando, K. Inomata, M. Kawasaki, K. Mukaida and T. T. Yanagida, *Phys. Rev. D* **97**, no.12, 123512 (2018) doi:10.1103/PhysRevD.97.123512 [arXiv:1711.08956 [astro-ph.CO]].
- [49] K. Ando, M. Kawasaki and H. Nakatsuka, *Phys. Rev. D* **98**, no.8, 083508 (2018) doi:10.1103/PhysRevD.98.083508 [arXiv:1805.07757 [astro-ph.CO]].
- [50] M. Kawasaki and H. Nakatsuka, *JCAP* **05**, 023 (2021) doi:10.1088/1475-7516/2021/05/023 [arXiv:2101.11244 [astro-ph.CO]].
- [51] M. Sasaki and E. D. Stewart, *Prog. Theor. Phys.* **95**, 71-78 (1996) doi:10.1143/PTP.95.71

- [arXiv:astro-ph/9507001 [astro-ph]].
- [52] C. Gordon and A. Lewis, Phys. Rev. D **67** (2003), 123513 doi:10.1103/PhysRevD.67.123513 [arXiv:astro-ph/0212248 [astro-ph]].
- [53] T. Kobayashi, Phys. Rev. Lett. **125**, no.1, 011302 (2020) doi:10.1103/PhysRevLett.125.011302 [arXiv:2005.01741 [astro-ph.CO]].
- [54] K. Dimopoulos, D. H. Lyth, A. Notari and A. Riotto, JHEP **07**, 053 (2003) doi:10.1088/1126-6708/2003/07/053 [arXiv:hep-ph/0304050 [hep-ph]].
- [55] P. Chingangbam and Q. G. Huang, JCAP **04**, 031 (2009) doi:10.1088/1475-7516/2009/04/031 [arXiv:0902.2619 [astro-ph.CO]].
- [56] N. Aghanim *et al.* [Planck], Astron. Astrophys. **641**, A6 (2020) [erratum: Astron. Astrophys. **652**, C4 (2021)] doi:10.1051/0004-6361/201833910 [arXiv:1807.06209 [astro-ph.CO]].
- [57] Y. Akrami *et al.* [Planck], Astron. Astrophys. **641**, A9 (2020) doi:10.1051/0004-6361/201935891 [arXiv:1905.05697 [astro-ph.CO]].
- [58] M. Kawasaki, K. Kohri and N. Sugiyama, Phys. Rev. D **62**, 023506 (2000) doi:10.1103/PhysRevD.62.023506 [arXiv:astro-ph/0002127 [astro-ph]].
- [59] M. Alvarez, T. Baldauf, J. R. Bond, N. Dalal, R. de Putter, O. Doré, D. Green, C. Hirata, Z. Huang and D. Huterer, *et al.* [arXiv:1412.4671 [astro-ph.CO]].
- [60] T. S. Bunch and P. C. W. Davies, “Quantum Field Theory In De Sitter Space: Renormalization By Point Splitting,” Proc. Roy. Soc. Lond. A **360** (1978) 117;
 A. Vilenkin and L. H. Ford, “Gravitational Effects Upon Cosmological Phase Transitions,” Phys. Rev. D **26**, 1231 (1982);
 A. D. Linde, “Scalar Field Fluctuations In Expanding Universe And The New Inflationary Universe Scenario,” Phys. Lett. B **116**, 335 (1982);
 A. A. Starobinsky and J. Yokoyama, “Equilibrium state of a selfinteracting scalar field in the De Sitter background,” Phys. Rev. D **50**, 6357 (1994) [arXiv:astro-ph/9407016].